LRG1 promotes angiogenesis by modulating endothelial TGFß signalling

Xiaomeng Wang[1], **Sabu Abraham**[1], **Jenny A.G. McKenzie**[1], **Natasha Jeffs**[1], **Matthew Swire**[1], **Vineeta B. Tripathi**[1], **Ulrich F.O. Luhmann**[2], **Clemens A.K. Lange**[2,3,4], **Zhenhua Zhai**[5], **Helen M. Arthur**[5], **James Bainbridge**[2,3], **Stephen E. Moss**[#1], and **John Greenwood**[#1]

[1]Department of Cell Biology, UCL Institute of Ophthalmology, London EC1V 9EL, UK.

[2]Department of Genetics, UCL Institute of Ophthalmology, London EC1V 9EL, UK.

[3]NIHR Biomedical Research Centre for Ophthalmology, Moorfields Eye Hospital, London, UK.

[4]University Eye Hospital Freiburg, Freiburg, Germany.

[5]Institute of Genetic Medicine, Newcastle University, UK.

[#] These authors contributed equally to this work.

Abstract

Aberrant neovascularisation contributes to diseases such as cancer, blindness and atherosclerosis and is the consequence of inappropriate angiogenic signalling. While many regulators of pathogenic angiogenesis have been identified, our understanding of this process is incomplete. Here we explored the transcriptome of retinal microvessels isolated from mouse models of retinal disease that exhibit vascular pathology and uncovered an up-regulated gene, leucine-rich alpha-2-glycoprotein-1 (*Lrg1*), of previously unknown function. We show that in the presence of TGF 1, LRG1 is mitogenic to endothelial cells and promotes angiogenesis. Mice lacking *Lrg1* develop a mild retinal vascular phenotype but exhibit a significant reduction in pathological ocular angiogenesis. LRG1 binds directly to the TGF accessory receptor endoglin which, in the presence of TGF 1, results in promotion of the pro-angiogenic Smad1/5/8 signalling pathway. LRG1 antibody blockade inhibits this switch and attenuates angiogenesis. These studies reveal a novel regulator of angiogenesis that mediates its effect through modulating TGF signalling.

The formation of new blood vessels by angiogenesis is a key feature of a number of diseases including age-related macular degeneration (AMD), proliferative diabetic retinopathy (PDR), atherosclerosis, rheumatoid arthritis and cancer. The factors that promote neovascularisation have been the subject of extensive research, with the vascular endothelial growth factors (VEGFs) and their receptors emerging as master regulators[1-3]. Despite the

prominent role of VEGF, other factors contribute to neoangiogenesis through coordinated crosstalk that is often highly context-dependent[4-6]. Such complexity is exemplified in transforming growth factor beta (TGF) 1 signalling, which can switch from being mostly angiostatic to pro-angiogenic[7]. What regulates this switch is not fully understood but activation of the pro-angiogenic pathway involves TGF receptor-II (T RII) recruitment of the predominantly endothelial TGF type I receptor, activin receptor-like kinase (ALK)1, which in turn initiates activation of the transcription factors Smad 1, 5 and 8 resulting in a pro-angiogenic phenotype[7-10]. The regulation of this differential signalling is contingent on multiple factors including the concentration of TGF , its bioavailability and the presence or absence of other regulatory factors such as bone morphogenic proteins (BMPs) and accessory receptors such as endoglin (ENG) and betaglycan[11].

Our incomplete understanding of the role of the fine-tuning of angiogenesis suggests that additional modulators have yet to be identified. Our objective in this study, therefore, was to identify novel regulators of pathogenic angiogenesis that may lead to the development of more effective treatment strategies.

Retinal vascular expression of LRG1

To identify novel regulators of neovascularisation we exploited three mouse mutants that exhibit marked remodelling of the retinal vasculature (Supplementary Fig 1 and Supplementary Movies 1 to 4). Genome-wide transcriptome analysis of retinal microvessel fragments isolated from the retinal dystrophy (RD)1 mouse, the very low density lipoprotein receptor (VLDLR) knockout mouse and the *Grhl3*[ct]/J curly tail mouse (The Jackson Laboratory) and appropriate wild type (WT) control mice yielded 62 genes that were differentially regulated but common to all three retinal disease models (Supplementary Table 1). When ranked according to fold change, a gene encoding a secreted glycoprotein of unknown function, namely leucine-rich alpha-2-glycoprotein-1 (*Lrg1*), emerged as the most significantly up-regulated. LRG1 is a highly conserved member of the leucine-rich repeat (LRR) family of proteins, many of which are involved in protein-protein interactions, signalling and cell adhesion (Supplementary Fig 2a and b).

Validation of the microarray data revealed that in the retina LRG1 is restricted almost exclusively to the vasculature, is expressed under normal conditions and is up-regulated during retinal vascular remodelling in the three mouse models of retinal disease (Fig 1a-d; Supplementary Fig 3). However, LRG1 expression was not restricted to the retina as we also observed LRG1 staining in the choriocapillaris of the mouse eye (Supplementary Fig 4a). Consistent with the data obtained in the mouse, we observed low levels of constitutive LRG1 expression in normal adult human retinal vessels and weakly, but not exclusively, in vessels in other human tissues including breast, skin and intestine (Supplementary Fig 4b).

We next investigated whether the *Lrg1* transcript is also increased in the retinae of models of choroidal and retinal neovascularisation. Choroidal neovascularisation (CNV) was induced in WT mice, and one week after laser injury we observed a significant increase in *Lrg1* transcript levels in both the retina and RPE/choroid (Figs 1e and 1f). We then examined intra-retinal/pre-retinal neovascularisation in the mouse model of oxygen-induced retinopathy (OIR), which displays hypoxia-driven retinal angiogenesis. At P17, during the ischaemic proliferative phase of OIR when neovascularisation is most prevalent, *Lrg1* transcript levels were also up-regulated (Fig 1g). However, at the end of the hyperoxic phase (P12) *Lrg1* mRNA was significantly reduced. Indeed, the pattern of *Lrg1* expression at the two time points observed mirrored the expression of the hypoxia-responsive genes *Vegfa*, *Apln* (Apelin) and its receptor *Aplnr* (Supplementary Fig 5). To determine whether LRG1 is up-regulated in human retinal disease in which there is neovascular pathology, vitreous

samples from human subjects with PDR were analysed by western blot which revealed increased LRG1 expression compared to control vitreous (Fig 1h; Supplementary Fig 6). It is unclear, however, whether this increase is the consequence of increased local production, leakage from the systemic circulation or a combination of both.

These data show that in the retina LRG1 expression is predominantly vascular, is constitutive and is increased during neovascular growth.

LRG1 and angiogenesis

To investigate the function of LRG1 we used cultured endothelial cell (EC) assays and *in vitro* and *ex vivo* models of angiogenesis. We observed that over-expression of *LRG1* in ECs increased proliferation whereas *Lrg1* knockdown decreased proliferation (Supplementary Fig 7). In addition, EC migration was inhibited by an anti-LRG1 polyclonal antibody (Supplementary Fig 7 and 8). In the Matrigel human umbilical vein EC (HUVEC) tube-formation assay, supplementation of media with recombinant human LRG1 (Supplementary Fig 8) caused a significant increase in tube formation and branching, whereas an anti-LRG1 antibody significantly blocked tube formation (Fig 2a; Supplementary Figs 8 and 9). Consistent with the latter observation, LRG1 was found to be present in the conditioned media of these assays (Supplementary Fig 10). We next investigated whether LRG1 promotes blood vessel growth in two *ex vivo* models of angiogenesis. Mouse metatarsals (E16.5) and aortic rings (P7) were prepared using tissues from WT mice. Vessel outgrowth and branching from explanted metatarsals (Supplementary Fig 11) or aortic rings in the absence of other added growth factors were significantly increased upon addition of exogenous LRG1 and inhibited in the presence of the anti-LRG1 polyclonal antibody (Fig 2b). Again, conditioned media from both assays was found to contain LRG1 protein (Supplementary Fig 10).

Having demonstrated that LRG1 influences vascular growth *in vitro* and *ex vivo* we then investigated the retinal vasculature of the *Lrg1* knock-out mouse (Supplementary Fig 12). *Lrg1*^{−/−} mice were viable but exhibited a delay in the development of the deep vascular plexus at P10 to P12 and the intermediate vessels between P17 and P25 that resolved by postnatal day 35 (Supplementary Fig 13). In addition, the hyaloid vessels failed to regress fully, with vessel persistence beyond P35 and integration into the inner retina (Supplementary Fig 14). Defective retinal vascular development and persistent hyaloid vessels were also reported in mice with deletions in *Ndp* (Norrin), *Fzd4* (Frizzled-4), *Lrp5* and *Angpt2* (angiopoietin-2) which also contribute to angiogenesis[12-14]. We also observed an increase in the incidence of cross-over of the radial arteries and veins and of their side branches, with occasional small vessels forming arteriovenous anastomosis (Supplementary Fig 15). Arteriovenous crossing has been reported in the retina of the hypomorphic *Vegfa* mouse[15] and is associated with susceptibility to branched vein occlusion in the human retina[16,17]. In this context it was interesting to note that *Vegfa* gene expression in the *Lrg1*^{−/−} mouse retina is significantly lower than in control mice in contrast to *Plgf* which is unchanged (Supplementary Fig 16). Aside from these mild defects, the retinal vasculature of the *Lrg1*^{−/−} mice exhibited similar pericyte coverage (Supplementary Fig 17) and barrier properties (Supplementary Fig 18) to WT controls.

As we had observed that LRG1 inhibition or supplementation had a significant effect on vessel formation in the metatarsal and aortic ring assays, we hypothesised that *Lrg1* knockout would lead to reduced angiogenesis in these models. Indeed, vessel formation was significantly reduced in *Lrg1*^{−/−} mice in both the metatarsal and aortic ring assay (Fig 2c; Supplementary Fig 19), and could be rescued by the addition of exogenous LRG1. Together

these data support the hypothesis that LRG1 contributes to, and is necessary for, robust vascular growth.

LRG1 and pathogenic neovascularisation

As our data thus far had demonstrated increased *Lrg1* transcript expression in CNV and OIR in WT mice we investigated whether neovascularisation in these models is attenuated in *Lrg1*$^{-/-}$ mice. CNV was induced in WT and *Lrg1*$^{-/-}$ mice, and at 7 days post-laser fundus fluorescein angiography (FFA) at 90 seconds revealed a diminished neovascular response in the *Lrg1*$^{-/-}$ mice compared to controls (Fig 3a; P<0.01). Concomitant with this was an equivalent reduction in fluorescein leakage at 7 minutes post injection. This effect was confirmed in a group of animals in which the neovascular lesion was visualised in posterior eyecup whole mounts, quantitative analysis of which showed that mean lesion size was ~70% smaller in *Lrg1*$^{-/-}$ than WT mice (Supplementary Fig 20). The reduction in lesion size in the *Lrg1*$^{-/-}$ mouse was similar to that reported in *Plgf*$^{-/-}$ [18] and *Ccr3*$^{-/-}$ [19] mice, two other pro-angiogenic factors, and could not be explained by changes in macrophage recruitment (Supplementary Fig 20) or pericyte coverage (Supplementary Fig 21). We next investigated intra-retinal/pre-retinal neovascularisation, as observed in PDR, in the OIR model of angiogenesis. Following the 5-day hyperoxia phase, the size of the avascular region at P12 was not significantly different between the *Lrg1*$^{-/-}$ and WT animals (Fig 3b; Supplementary Fig 22). Furthermore, after 5 days in normoxia revascularisation of the avascular region with ordered vessels was similar between the two groups, demonstrating that hyperoxia-induced regression and hypoxia-induced physiological revascularisation are not affected by the loss of LRG1. However, the area occupied by disordered neovascular growth (tufts) was significantly reduced in the absence of LRG1 (Fig 3b; P<0.01; Supplementary Fig 22), demonstrating that LRG1 is specifically required for robust pathogenic angiogenesis.

Having demonstrated that an antibody against LRG1 inhibits angiogenesis *in vitro* we investigated whether this antibody would also reduce CNV lesion size. Following the laser burn, animals received intravitreal injections of the anti-LRG1 polyclonal antibody or a pre-immune IgG as control, and 5 days later lesion sizes were measured. In the anti-LRG1 antibody-treated eyes a dose-dependent reduction in CNV lesion volume (Fig 3c and d) and area (Supplementary Fig 23) was observed compared to control antibody-treated eyes. Indeed, the 58% reduction of CNV volume (Fig 3d) and 46% reduction in area at a dose of 10μg (Supplementary Fig 23) was of similar magnitude as that achieved with blockade of the VEGF/PlGF signalling axis[20] or the chemokine receptor CCR3[19].

As antibody blockade of LRG1 reduces CNV lesion size we investigated the effects of combination therapy with a VEGF receptor 2 (VEGFR2)-blocking antibody[20]. Antibody blockade of LRG1 alone, VEGFR2 alone, or both LRG1 and VEGFR2 inhibited CNV lesion volume (Fig 3e; Supplementary Fig 23) with the combined therapy giving the most significant inhibition. The effect of combinatorial treatment was also evaluated in OIR. Under the treatment conditions employed, where the individual antibodies elicited no significant effect, animals treated with the antibody combination exhibited a significant inhibition of both patterned revascularisation and the formation of pathogenic vascular tufts (Supplementary Fig 24). These data provide compelling evidence that inhibition of LRG1 is effective in preventing pathological angiogenesis and suggest that LRG1 has potential as a therapeutic target on its own or in combination with other anti-angiogenic therapies.

LRG1 and TGFß signalling

Whilst little is known regarding the biology of LRG1, concomitant increases in the expression levels of TGFβ1, TβRII and LRG1 have been reported in cancer cells[21] and

hydrocephalus[22], and LRG1 has been shown to bind to TGFβ1 in high endothelial venules[23]. Consistent with this, and with earlier proteomic and transcriptome analyses[24,25], we have shown here that in vitreous samples from the eyes of human subjects with PDR, both LRG1 (Fig 1h; Supplementary Fig 6) and TGFβ1 (Supplementary Fig 25) are significantly increased. Furthermore, alongside increased *Lrg1*, *Tgfb1* transcript levels were also significantly up-regulated in the retinae of laser-induced CNV mice and in OIR mice during the ischaemic proliferative phase (Supplementary Fig 5). These data prompted us to investigate whether LRG1 acts as a modulator of TGFβ signalling.

To determine whether LRG1 associates with components of the TGFβ receptor complex we performed co-immunoprecipitation experiments. In primary brain ECs LRG1 was present in immunoprecipitates of TβRII, ALK1, ALK5 and the auxiliary receptor ENG (Fig 4a). Conversely, immunoprecipitates of LRG1 from HUVEC were found to contain TβRII, ALK1, ALK5 and ENG (Supplementary Fig 26a). These observations suggested that LRG1 might be involved in regulating TGFβ signalling through fine-tuning the stoichiometry of the TGFβ receptor complex. TGFβ1 signals in ECs through TβRII recruiting either the ubiquitous ALK5 receptor or the predominantly endothelial ALK1 receptor, either on its own or together with ALK5. Stimulation of the TβRII/ALK5 signalling complex results in phosphorylation and activation of the transcription factors Smad 2 and 3, which increases extracellular matrix deposition, inhibits EC proliferation and migration, and promotes cell homeostasis, whilst TβRII/ALK5/ALK1 signalling, possibly in association with ENG, activates Smads 1, 5 and 8 resulting in a pro-angiogenic state[7,8]. We therefore investigated the direct one-to-one binding of LRG1 to recombinant extracellular domains of individual TGFβ receptors in serum-free conditioned media from transfected HEK 293 cells (Supplementary Fig 26b). Immunoprecipitation of the receptor ectodomain revealed coimmunoprecipitation of LRG1 with ALK5, TβRII and ENG indicating a direct interaction of LRG1 with these individual receptors (Fig 4b). This occurred in the absence of TGFβ1, which was not present in HEK 293 cell conditioned medium (Supplementary Fig 10). Addition of conditioned medium containing non-tagged ENG, ALK5 or TβRII out-competed tagged receptor binding to LRG1 (Fig 4c) confirming the specificity of these protein-protein interactions. The observation that ENG appears to be one of the receptors for LRG1 is germane, given its proposed role in switching TGFβ signalling towards the pro-angiogenic Smad1/5/8 pathway. A potential functional relationship between LRG1 and ENG was additionally strengthened by our observation that *Eng* is up-regulated in CNV and OIR (Supplementary Fig 27). To further define the LRG1-ENG interaction we undertook surface plasmon resonance analysis (BIAcore) and obtained an affinity rate constant (K_D) of 2.9 μM (Supplementary Fig 28) for binding of the ENG ectodomain to LRG1.

These data raise the possibility that LRG1 facilitates a receptor configuration conducive to the pro-angiogenic signalling pathway. To investigate this, LRG1 was incubated with conditioned media containing the extracellular domains of either ALK1 or ALK5 in the presence or absence of different combinations of TGFβ1 and the extracellular domains of ENG and TβRII. These studies revealed that LRG1 only associated with ALK1 in the presence of ENG, to which it bound, and this was enhanced by the addition of TGFβ1 (Fig 4d). Conversely, ALK5 binds LRG1 in the absence of ENG but in its presence this interaction is attenuated, suggesting competition between ENG and ALK5 for LRG1, whilst the addition of TGFβ1 results in complete loss of the LRG1-ALK5 association. Moreover, neither TGFβ1 nor TβRII on their own, nor a combination of both, affects ALK1-LRG1 or ALK5-LRG1 association in the absence of ENG. However, in the presence of ENG, TβRII is able to form a complex with ALK1-LRG1 or ALK5-LRG1, with the former association being enhanced and the latter being further inhibited by TGFβ1. In accordance with previously suggested models[8], these data imply that LRG1 may be able to form an intermediate complex with ALK5, ALK1, TβRII and ENG but that in the presence of

TGFβ1 the LRG1/ALK1/TβRII/ENG complex predominates. An association between LRG1 and TGFβ1 may therefore lead to more efficient ALK1/TβRII/ENG receptor complex formation and consequently to the promotion of pro-angiogenic Smad1/5 signalling.

To test this hypothesis we treated mouse brain ECs with TGFβ1 (5ng/ml) and showed that both Smad2/3 and Smad1/5 phosphorylation are induced in WT cells but in *Lrg1* null cells only Smad2/3 is activated (Fig 5a). The addition of LRG1 alone did not activate Smad2/3 or Smad1/5, but in combination with TGFβ1 there was a dramatic induction of Smad1/5 phosphorylation showing that LRG1 requires the presence of TGFβ1 to stimulate the pro-angiogenic TβRII-ALK1-Smad1/5/8 pathway (Fig 5a). As TGFβ1 is an EC mitogen[7] we also investigated whether LRG1 augmented TGFβ1-mediated cell proliferation. Brain ECs from *Lrg1*^{−/−} mice proliferated more slowly than those from WT animals (Fig 5b). Addition of TGFβ1 significantly enhanced EC proliferation from WT animals but inhibited the growth of cells from *Lrg1*^{−/−} mice, presumably through enhanced ALK5-Smad2/3 signalling in the absence of activation of the ALK1-Smad1/5/8 arm. The addition of LRG1 on its own had no effect, but TGFβ1 and LRG1 in combination increased proliferation significantly in both WT and *Lrg1* null ECs (Fig 5b). Moreover, in the metatarsal angiogenesis assay the combined addition of LRG1 and TGFβ1 led to a substantial increase in vessel formation (Fig 5c). The observation that LRG1 alone induced a small increase in vessel formation implies that TGFß1 is produced constitutively by the metatarsal tissue, which was confirmed by western blotting of conditioned medium (Supplementary Fig 10).

To confirm that the pro-angiogenic effect of LRG1 was mediated through the ALK1-Smad1/5/8 pathway, ALK1 was knocked down with siRNA (Fig 5d; Supplementary Fig 29) or inhibited with LDN193189 (Supplementary Fig 29), resulting in prevention of LRG1-induced Smad1/5 phosphorylation without affecting Smad2 phosphorylation. As predicted, in the Matrigel assay ALK1 inhibition led to a significant decrease in HUVEC tube and branch formation and blocked the angiogenic activity of LRG1 in this assay (Fig 5f; Supplementary Fig 29). Conversely, knockdown of ALK5 with siRNA (Figs 5d and f) or inhibition with SB43152 (Supplementary Fig 29), which inhibited constitutive Smad2 phosphorylation, did not prevent LRG1-induced HUVEC tube formation. siRNA knockdown of TβRII or ENG also resulted in the abrogation of LRG1-induced Smad1/5 phosphorylation (Fig 5e; Supplementary Fig 29) and HUVEC tube and branch formation (Fig 5g). To further corroborate the involvement of ENG in LRG1-mediated signalling, lung ECs derived from *Rosa26-CreERT:Eng*^{fl/fl} mice[26] were treated with 4OH-tamoxifen to deplete ENG (MLEC;*Eng*^{−/−}) (Fig 5h). Unlike control cells, treatment of MLEC;*Eng*^{−/−} with a combination of TGFβ1 and LRG1 failed to induce Smad 1/5 phosphorylation (Fig 5h). Consistent with this, similar treatment resulted in a significant increase in control cell division whilst that of MLEC;*Eng*^{−/−} was significantly reduced and refractive to treatment with TGFβ1 ± LRG1 (Fig 5i). In addition, we employed an endothelial-specific conditional knockout approach in which metatarsals were harvested from *Eng*-floxed mice (*Cdh5(PAC)-CreERT2;Eng*^{fl/fl})[27] and treated with 4OH-tamoxifen (to generate Eng-iKO[e] metatarsals). This resulted in a loss of vascular ENG expression, compared to *Eng*^{fl/fl} controls (Supplementary Fig 30), and a 51% reduction in LRG1-induced vessel growth (*P*<0.01; Fig 5j) and a 53% reduction in vessel branching (*P*<0.05; Fig 5k). In agreement with these data, there were fewer pSmad1/5/8 positive cells in CNV lesions in *Lrg1*^{−/−} mice compared to WT animals (Supplementary Fig 31). Moreover, in both CNV and OIR (during the neovascular phase) the Smad1/5 mediated pro-mitogenic gene inhibitor of DNA binding 1 (*Id1*) was significantly up-regulated (Supplementary Fig 5).

Conclusions

TGF signalling plays an important role in determining EC function during both development and vascular pathology[7,8,28,29] and its activity is regulated at multiple levels from gene expression to control of extracellular bioavailability. The multiplicity of regulatory mechanisms together with variable combinations of receptors/co-receptors creates complex patterns of TGF activity that define its context-dependent effects. In particular, the balance between the ALK5 and ALK1 signalling pathways is considered to be central in determining the angiogenic switch with ENG being proposed as a key regulatory molecule in promoting signalling through the ALK1 pathway[29-31]. In searching for mediators of vascular remodelling in the diseased/damaged retina we have discovered a novel regulator of TGFß signalling. The data presented here support a hypothesis that LRG1 activates the TGF angiogenic switch by binding to the accessory receptor ENG and, in the presence of TGF 1, promotes signalling via the T RII-ALK1-Smad1/5/8 pathway (Supplementary Fig 32). Moreover, our evidence suggests that LRG1 may play a more dominant role in disorganised pathological rather than developmental/physiological angiogenesis. Whilst in the retina this is clearly supported by our *in vivo* data, the *ex vivo* and *in vitro* studies indicate that LRG1 angiogenic activity is not restricted to the eye. The modulating effect of LRG1 on TGFß1 signalling is the first demonstration of a definitive function for LRG1 and raises the intriguing possibility that it may influence other major biological processes in which TGFß plays a role including neoplasia[32] and the immune response[33]. Inhibition of LRG1, which we show here causes a shift away from angiogenic signalling, could present an alternative way of preventing pathogenic activation of this pathway, whilst leaving homeostatic ALK1 signalling unperturbed. From these studies we suggest, therefore, that LRG1 is a highly promising therapeutic target for controlling pathogenic angiogenesis in ocular disease, and potentially in other diseases such as cancer and atherosclerosis.

Methods

Animals

C57/BL6 mice were purchased from Harlan laboratories (Blackthorn, UK). RD1[34], *Vldlr*[−/− 35], and *Grhl3*[ct]/J curly tail mice were purchased from the Jackson Laboratory (Maine, USA). *Lrg1*^{−/−} mice were generated by the knockout mouse project (KOMP) repository (University of California Davies, USA) (http://www.komp.org/ and Supplementary Fig 12). *Rosa26-CreERT;Eng*^{fl/fl} and *Cdh5(PAC)- CreERT2;Eng*^{fl/fl} mice have been previously described[26,27]. All procedures were performed in accordance with the UK Animals (Scientific Procedures) Act and with the Association for Research in Vision and Ophthalmology Statement for the Use of Animals in Ophthalmic and Vision Research and the Animal Welfare and the Ethical Review Bodies of the UCL Institute of Ophthalmology and Newcastle University.

Vessel isolation and gene expression analysis

Mouse retinal vessels from wild type C57BL/6J (15 weeks), *Vldlr*^{−/−} (16 weeks), RD1 (18 weeks) and *Grhl3*[ct]/J curly tail (13 weeks) mice were isolated as described elsewhere[36]. RNA was extracted from the enriched microvascular preparations and processed for whole genome microarray analysis as previously described[36]. Twelve mice were used per strain per RNA extraction. This was repeated four times providing RNA for 4 chips per animal model.

Quantitative real-time PCR

RNA was extracted using Trizol (Invitrogen, Paisley, UK) followed by an RNeasy clean-up (QIAGEN, Crawley, UK, West Sussex, UK). RNA was reverse transcribed using the QuantiTect Reverse Transcription Kit (QIAGEN, Crawley, UK) and PCR was conducted with QuantiTect PowerSybr Green (Applied Biosystems, Paisley, UK) using a 7900HT Fast Real-Time PCR System (Applied Biosystems, Paisley, UK); samples were normalised to glyceraldehyde-3-phosphate dehydrogenase (*Gapdh*). Primers used in this study are listed in Supplementary Table 2. Student's t test was performed to determine statistical significance between test groups.

SDS-PAGE and western blotting

Proteins were separated by SDS-PAGE. Gels were either stained using Coomassie-blue or transferred onto a Hybond-P PVDF membrane (GE Healthcare, Buckinghamshire, UK). Blots were probed with phospho-Smad1/5 antibody (Rabbit mAb, NEB, Hertfordshire, UK), phospho-Smad2 antibody (Rabbit mAb, NEB, Hertfordshire, UK), TGFβ1 antibody (mouse monoclonal, R&D systems, Abingdon, UK), TβRII antibody (mouse monoclonal, R&D systems, Abingdon, UK), ALK1 antibody (rabbit polyclonal, Santa Cruz Biotechnology, Heidelberg, Germany), ALK5 antibody (rabbit polyclonal, Abcam, Cambridge, UK), endoglin antibody (mouse monoclonal, R&D Systems, Abingdon, UK), LRG1 antibody (HPA001888, rabbit polyclonal, Sigma, UK) or GAPDH antibody (mouse monoclonal, Novus, Cambridge, UK) followed by HRP-conjugated secondary antibodies (GE Healthcare, Buckinghamshire, UK) or HRP-conjugated Protein A (GE Healthcare, Buckinghamshire, UK). Densitometry was performed using ImageJ software (National Institute of Health). Student's t test was performed to determine statistical significance between test groups.

RNA *in situ* hybridization (ISH)

Eyes were fixed in 2% (w/v) paraformaldehyde (PFA) in PBS for 2 min and dissected in 2 x PBS. Retinae were flattened and fixed in 100% ice-cold methanol overnight at −20°C. After recovery from methanol, retinae were re-fixed for 10 min in 4% PFA and washed in PBS before digestion for 10 min in proteinase K (80μg/ml in PBS). Retinae were re-fixed for 5 min in 4% PFA and 0.2% glutaraldehyde in PBS. After a brief wash in PBS, retinae were pre-incubated in hybridization buffer (50% formamide, 5 x SSC, 50μg/ml tRNA, 1% SDS, 50μg/ml Heparin) for 1 h at 65°C. Denatured RNA probes were incubated with retinae at 65°C overnight. Primers used to generate RNA probes by PCR are listed in Supplementary Table 2. Probes were labelled with digoxigenin-UTP using a DIG RNA labelling kit (Roche diagnostics, Burgess Hill, UK). Signal was developed with alkaline phosphatase-conjugated anti-digoxigenin Fab fragments, according to the manufacturer's instructions.

Immunohistochemistry

Retinal/RPE whole mounts were fixed and stained as previously described[37] and incubated overnight with antibodies against human LRG1 (HPA001888), mouse PECAM-1 (Rat monoclonal, BD Biosciences, Oxford, UK), mouse Collagen IV (rabbit polyclonal, AbD Serotec, Kidlington, UK), human Collagen IV (goat polyclonal, Millipore, Watford, UK), rat NG2 (rabbit polyclonal, Millipore), mouse F4/80 (rat monoclonal, AbD Serotec), mouse endoglin (rat monoclonal, Santa Cruz Biotechnology, Santa Cruz, USA) or human VE-Cadherin (mouse monoclonal, Santa Cruz Biotechnology) and identified with Alexa 488, Alexa 594 or Alexa 647 secondary antibodies (Invitrogen, Paisley, UK) or FITC-GSL isolectin IB4 (Vector Labs, Peterborough, UK). Retinae were flat-mounted in Mowiol and examined by epifluorescence (Leica DM IRB inverted research microscope or Olympus *SZX16* Research stereo zoom *microscope*) or confocal (Carl *Zeiss* LSM 510 or *710*)

microscopy. For quantifying the retinal vascular area, raw image data were processed with Photoshop CS4.3. Three-dimensional rendering of confocal Z stacks was carried out using Imaris 7.5 software (Bitplane AG, Switzerland). The retinal vasculature was analysed through automatic surface rendering aided by manual threshold adjustment so that only blood vessels were included for analysis. Imaris Key Frame Animation was used for movie generation.

Human tissue

Vitreous and plasma samples were collected from patients having surgery for proliferative diabetic retinopathy (PDR) or epiretinal membrane. Human tissue arrays were obtained from Pantomics (Richmond, CA, USA) and stained with rabbit anti-LRG1 antibody (Sigma, Dorset, UK). The study followed the ethical guidelines of the Declaration of Helsinki. Institutional review boards granted approval for allocation and biochemical analysis of specimens.

Cells and cell culture

Pooled human umbilical vein endothelial cells (HUVEC) were purchased from Lonza (Slough, UK) and cultured according to suppliers instructions. HEK293T cells were purchased from Invitrogen (Paisley, UK) and cultured as recommended. Mouse primary brain endothelial cells were isolated, purified and cultured as previously described for rat[38]. The immortalized Lewis rat brain microvascular endothelial cell line GPNT was grown as previously described[39]. Mouse lung endothelial cells (MLEC) were isolated from *Rosa26-CreERT;Eng*$^{fl/fl}$ mice carrying the Immortomouse transgene and were harvested and cultured as previously described[26]. Cells were pre-treated with 1μM 4OH-tamoxifen for 48 h in culture to generate ENG-depleted cells (MLEC;*Eng*$^{-/-}$) and untreated cells served as controls (MLEC;*Eng*$^{fl/fl}$).

Generation of LRG1 polyclonal antibody

Rabbits were immunised with purified full-length His-tagged human LRG1 protein (Covalab, UK). Preimmune sera were collected to produce control IgG. Antisera were collected after 3 months and antibody was purified by HiTrap Protein G FF column (GE Healthcare) and concentrated and desalted using HiPrep 26/10 Desalting (GE Healthcare).

Matrigel human umbilical vein endothelial cell (HUVEC) tube formation assay

HUVEC were grown on Growth Factor-Reduced Matrigel (BD Biosciences, Oxford, UK) as described elsewhere[40]. 96-well plates were coated with Matrigel containing diluent (control) or LRG1 (20μg/ml), rabbit polyclonal antibody against LRG1 (C10-54) (100nM), rabbit IgG (100nM), ALK1 inhibitor (LDN 193189, Axon Medchem BV, Groningen, Netherlands, 100nM) or ALK5 inhibitor (SB43152, Sigma, Dorset, UK, 10μM) and allowed to polymerize in the incubator at 37°C for 45 min. Tube formation was visualized using an Olympus *SZX16* Research stereomicroscope and analysed by counting the number of branch points and total tube length per well using ImageJ. Three independent experiments were carried out and each was performed in triplicate. Student's t test was performed to determine statistical significance between test groups.

Metatarsal angiogenesis assay

The metatarsal angiogenesis assay was carried out as described[41]. Metatarsal bones were isolated from E16.5 WT control or *Lrg1*$^{-/-}$ littermate mice and treated with TGFβ1 (5ng/ml, R&D systems, Abingdon, UK), LRG1 (20μg/ml), anti-LRG1 polyclonal antibody (100nM) or rabbit IgG (100nM) as indicated. Medium was replaced every 2 days. At day 10 of culture, the explants were fixed and stained for PECAM-1 (rat monoclonal, BD Biosciences,

Oxford, UK) and visualized under an Olympus *SZX16* Research stereo zoom microscope. Following image processing in Photoshop CS4 to mask the cartilage, the length of PECAM-1-positive tubular structures and the number of branch points were determined by Imaris 7.5 software (Bitplane) using automatic filament tracing with manual threshold corrections. Statistical data were imported into Excel (Microsoft) for calculating total vessel length and the number of branch points. A least three independent experiments were carried out comprising a minimum of 30 metatarsals for each treatment. Student's t test was performed to determine statistical significance between test groups.

To investigate the effect of ENG depletion on the pro-angiogenic effect of LRG1, metatarsals from *Cdh5(PAC)-CreERT2;Eng^{fl/fl}* mice[27] were used to generate endothelial-specific depletion of ENG following addition of 1μM 4OH-tamoxifen 3 days after metatarsal bone isolation, when neovessels began to emerge. On day 4, LRG1 was added to a final concentration of 20μg/ml and the media (including LRG1 and 4OH-Tamoxifen supplements) was refreshed every other day until day 12. ENG depletion was confirmed using an anti-ENG antibody (E-Bioscience). Separate experiments using control metatarsals confirmed that 1μM 4OH-tamoxifen *per se* did not affect neovessel formation in the metatarsal angiogenesis assay. Analysis of angiogenesis was carried out as described above. Metatarsals from 5 independent litters was used and two-way ANOVA was performed to determine statistical significance between test groups,

Aortic ring angiogenesis assay

The aortic ring angiogenesis assay was performed using the modified method of Nicosia and Ottinetti[42]. 1mm diameter rings were sliced from aortae of 2 week WT control or *Lrg1^{−/−}* littermate mice. Aortic rings were then placed in a 96-well plate coated with a rat tail collagen I gel (BD Biosciences, Oxford, UK) containing LRG1 (20μg/ml), anti-LRG1 polyclonal antibody (100nM) or rabbit IgG (100nM) as indicated, and cultured in DMEM supplemented with 2.5% FBS containing relevant compounds. Medium was replaced every 2 days. At day 10 of culture, the explants were fixed, stained for GSL isolectin IB4 (Vector Labs, Peterborough, UK) and visualized under an Olympus *SZX16* Research stereo zoom microscope. The number of sprouts was counted manually. Three independent experiments were carried out with a mean of 15 aortic rings being analysed for each treatment. Student's t test was performed to determine statistical significance between test groups.

Mouse model of choroidal neovascularization (CNV)

CNV was induced as described elsewhere[36,43]. In the anti-LRG1 antibody blockade study animals received an intravitreal injection of immediately following the laser burn. Antibody at a concentration of 1μg, 2.5μg, 5μg or 10μg (each in 1μl) of the anti-LRG1 polyclonal antibody was delivered to one eye and a pre-immune IgG, serving as control, delivered to the contralateral eye. Five (in the case of antibody treatment) or seven days after injury, CNV lesions were imaged as described before[36,43,44]. Mice were then killed for retina and RPE flatmount preparation and mRNA extraction. The CNV lesions were visualized following FITC-conjugated GSL isolectin B4 (Vector labs, Peterborough, UK) and mouse PECAM-1 (rat polyclonal, BD Biosciences, Oxford, UK) staining using an Olympus *SZX16* Research stereo zoom microscope and a Zeiss LSM 710 confocal microscope. Student's t test was performed to determine the statistical significance between WT and Lrg1 knockout mice. One way ANOVA was used to test statistical significance between antibody treatment groups.

Mouse model of oxygen-induced retinopathy (OIR)

Nursing mothers and neonatal mice were placed in a 75% oxygen supply chamber from postnatal day (P)7 to P12 and exposed to a standard 12 h light-dark cycle as previously

described[45]. The extent of vaso-obliteration was determined in retinal flatmounts at P12 and the extent of normal vessel regrowth and neovascularisation were evaluated at P17 as previously described[46]. Retinae were also recovered for mRNA extraction and analysis at P12 and P17. The effect of antibody blockade on retinal revascularisation and neovascular tuft formation was carried out by delivering anti-LRG1 blocking antibody (50mg/kg intraperitoneal in 100μl at P13 and P15), anti-VEGFR2 blocking antibody (DC101, 12.5mg/kg intraperitoneal at P13 and P15) or a combination of the two, followed by assessment of the vasculature at P17. Student's t test was performed to determine the statistical significance between WT and Lrg1 knockout mice. One way ANOVA was used to test statistical significance between antibody treatment groups.

Co-immunoprecipitation

Primary mouse brain EC from WT or $Lrg1^{-/-}$ littermate mice, GPNT cells or HUVEC were lysed in RIPA buffer (50 mM Tris-HCL pH7.5, 150 mM NaCl, 0.1% SDS, 0.5 % sodium deoxycholate and 1% Nonidet P-40). Soluble peptide-tagged extracellular domains of TβRII (Myc-tagged), ALK1 (HA-tagged), ALK5 (HA-tagged) and ENG (V5-tagged), as well as full length LRG1 (His-tagged), were generated in separate cultures of transfected HEK 293 cells, and serum-free media containing the individual proteins was harvested after 5 days. Non-tagged secreted extracellular domains of the TGFβ receptors were also generated in an identical manner. Media containing individual extracellular domains of a TGFβ receptor were incubated with media containing LRG1 in the presence or absence of TGFβ1 at 4°C with rotation prior to immunoprecipitation. After pre-clearing, cell lysates or recombinant protein mixtures were incubated with TGFβ receptor antibodies or anti-LRG1 antibody-conjugated protein G beads at 4°C overnight and then fractionated by SDS-PAGE and blotted. The membranes were probed with antisera as described earlier.

Proliferation assay

Mouse primary brain EC from $Lrg1^{-/-}$ and WT mice were cultured in EGM2 media supplemented with puromycin (5μg/ml) until sub-confluent, followed by 48 h serum starvation in EBM2 medium. Cells were stimulated with TGFβ1 (5ng/ml), LRG1 (20μg/ml) or TGFβ1 plus LRG1 in EBM2 medium at 37°C. After 3 h, cells were fixed and stained with an antibody to Ki67 (mouse mAb, Dako, Cambridge, UK) to detect proliferating cells. The proliferation rate was evaluated as the percentage of Ki67 positive cells of the total endothelial cell number per well. Student's t test was performed to determine the statistical significance between treatment groups.

Molecular biological methods

The coding sequence of human *LRG1* (NM_052972) carrying a 6 x His tag or HA tag at the 3′ end and Kozak consensus sequence at the 5′ end was cloned into pcDNA3.1 (Invitrogen, Paisley, UK) at the HindIII/XhoI sites to form pcDNA-LRG1-His or pcDNA-LRG1-HA (Supplementary Fig 8). The coding sequence of human LRG1 was cloned into pEGX4T1 GST expression vector (GE Healthcare) at the BamHI/SalI site to form GST-ENG. The extracellular domain of human TβRII (NM_001024847.2) carrying a Myc tag, ALK1 (NM_000020.2) carrying a HA tag, ALK5 (NM_004612.2) carrying a HA tag, ENG (NM_001114753.1) carrying a V5 tag at the 3′ end and Kozak consensus sequence at the 5′ end were cloned into pcDNA3.1 at HindIII/EcoRI sites. The recombinant human proteins were expressed in HEK293 cells (Invitrogen, Paisley, UK). siRNA oligos (SASI_Rn01_00111211 (Sigma)) were used for *Lrg1* gene knockdown in GPNT cells, and siRNA oligos (ON-TARGETplus SMARTpools, Thermo Scientific, Erembodegem, Belgium) were used for knockdown in HUVEC of *ALK1* (L-005302-00-0005), *ALK5* (L-003929-00-0005), *ENG* (L-011026-00-0005) and *TβRII* (L-001000-00-50) and control siRNA (D-001810-10-05) was used as a negative control for knockdown in HUVEC.

Lipofectamine™ 2000 transfection reagent (Invitrogen, Paisley, UK) was *used for transfection of mammalian cells.* Oligofectamine™ 2000 Transfection Reagent (Invitrogen, Paisley, UK) was used for siRNA knockdown in GPNT cells. GeneFECTOR transfection reagent (VennNova, Florida, USA) was used for siRNA knockdown in HUVEC. PCR and RT-PCR primer sequences are shown in Supplementary Table 2.

Purification of recombinant proteins

LRG1-His was expressed in HEK293 cells and purified using HisPrep FF16/10 column (GE healthcare) and buffer exchanged into PBS using HiPrep 26/10 Desalting (GE Healthcare) according to manufacturer's instruction. GST-ENG was expressed in BL21 competent cells and purified using *Glutathione* Sepharose 4B (GE Healthcare) and eluted in elution buffer (50 mM Tris-HCl, 10 mM reduced glutathione, pH 8.0) according to the manufacturer's instruction. Denatured LRG1-His protein (DLRG1) was generated by boiling at 100°C for 15 mins.

Surface plasmon resonance

All surface plasmon resonance experiments were carried out on a BiacoreT200 instrument (GE Healthcare). LRG1 was covalently immobilized via primary amino groups on a CM5 sensor chip as per manufacturer's instructions (specific contact time 20 s at a flow rate of 10 μl/min; LRG1 concentration at 25 μg/ml diluted using 10 mM sodium acetate pH 5.0). The amount of immobilized LRG1 corresponded to 2000 Response Units (RU) in flow cell 2. Flow cell 1 on the same sensor chip, reserved for control runs, was treated identically but without LRG1 immobilization. For all SPR measurements, GST-tagged ENG was diluted in running buffer (1 x PBS, pH 7.2). The association was monitored by injecting different concentrations (1-50 nM) of the analyte (ENG) into channels 1 and 2 starting with the lowest analyte concentration. All experiments were conducted in triplicates at 25°C at a flow rate of 30 μl/min. The association time for ligand-analyte steady state binding was optimised to 180 s and a subsequent 300 s were allowed for dissociation. Between injections the sensor chip surface was regenerated with Glycine HCl pH 2.0 at a flow rate of 30 μl/minute for 30 s. All curves were corrected for non-specific binding by subtraction of control curves obtained from injection of the analyte through the blank flow cell 1. The affinity and dissociation constants were calculated from the plots of the steady-state binding as a function of protein concentration, using the Biacore T200 evaluation software and a homogenous 1:1 Langmuir binding kinetic model. The analysis provided values for the dissociation affinity constant (K_D), the association rate constant (K_a) and the dissociation rate constant (K_d).

Statistical analyses

Data are represented as means ± s.e.m. Statistical analyses were performed by Student's *t* test or one-way ANOVA followed by Tukey/Bonferroni post-test analysis or two-way ANOVA as appropriate using Prism 5 (GraphPAD Software Inc.). *P* values of <0.05 are designated with one (*) asterisks, *P* values of <0.01 are designated with two (**) asterisks and *P* values of <0.001 are designated with three (***) asterisks. Each represents significant statistical comparisons among the listed (x axis) experimental groups.

Supplementary Material

Refer to Web version on PubMed Central for supplementary material.

Acknowledgments

References

1. Leung DW, Cachianes G, Kuang WJ, Goeddel DV, Ferrara N. Vascular endothelial growth factor is a secreted angiogenic mitogen. Science. 1989; 246:1306–1309. [PubMed: 2479986]

2. Carmeliet P, et al. Abnormal blood vessel development and lethality in embryos lacking a single VEGF allele. Nature. 1996; 380:435–439. [PubMed: 8602241]

3. Ferrara N, et al. Heterozygous embryonic lethality induced by targeted inactivation of the VEGF gene. Nature. 1996; 380:439–442. [PubMed: 8602242]

4. Holderfield MT, Hughes CC. Crosstalk between vascular endothelial growth factor, notch, and transforming growth factor-beta in vascular morphogenesis. Circ Res. 2008; 102:637–652. [PubMed: 18369162]

5. Chung AS, Ferrara N. Developmental and pathological angiogenesis. Annu Rev Cell Dev Biol. 2010

6. Carmeliet P, Jain RK. Molecular mechanisms and clinical applications of angiogenesis. Nature. 2011; 473:298–307. [PubMed: 21593862]

7. Pardali E, Goumans MJ, ten Dijke P. Signaling by members of the TGF-beta family in vascular morphogenesis and disease. Trends Cell Biol. 2010; 20:556–567. [PubMed: 20656490]

8. Goumans MJ, Liu Z, ten Dijke P. TGF-beta signaling in vascular biology and dysfunction. Cell Res. 2009; 19:116–127. [PubMed: 19114994]

9. Cunha SI, et al. Genetic and pharmacological targeting of activin receptor-like kinase 1 impairs tumor growth and angiogenesis. J Exp Med. 2010; 207:85–100. [PubMed: 20065063]

10. Cunha SI, Pietras K. ALK1 as an emerging target for antiangiogenic therapy of cancer. Blood. 2011; 117:6999–7006. [PubMed: 21467543]

11. ten Dijke P, Arthur HM. Extracellular control of TGFbeta signalling in vascular development and disease. Nat Rev Mol Cell Biol. 2007; 8:857–869. [PubMed: 17895899]

12. Xu Q, et al. Vascular development in the retina and inner ear: control by Norrin and Frizzled-4, a high-affinity ligand-receptor pair. Cell. 2004; 116:883–895. [PubMed: 15035989]

13. Ye X, et al. Norrin, frizzled-4, and Lrp5 signaling in endothelial cells controls a genetic program for retinal vascularization. Cell. 2009; 139:285–298. [PubMed: 19837032]

14. Hackett SF, Wiegand S, Yancopoulos G, Campochiaro PA. Angiopoietin-2 plays an important role in retinal angiogenesis. J Cell Physiol. 2002; 192:182–187. [PubMed: 12115724]

15. Haigh JJ, et al. Cortical and retinal defects caused by dosage-dependent reductions in VEGF-A paracrine signaling. Dev Biol. 2003; 262:225–241. [PubMed: 14550787]

16. Zhao J, Sastry SM, Sperduto RD, Chew EY, Remaley NA. Arteriovenous crossing patterns in branch retinal vein occlusion. The Eye Disease Case-Control Study Group. Ophthalmology. 1993; 100:423–428. [PubMed: 8460014]

17. Kumar B, et al. The distribution of angioarchitectural changes within the vicinity of the arteriovenous crossing in branch retinal vein occlusion. Ophthalmology. 1998; 105:424–427. [PubMed: 9499771]

18. Rakic JM, et al. Placental growth factor, a member of the VEGF family, contributes to the development of choroidal neovascularization. Invest Ophthalmol Vis Sci. 2003; 44:3186–3193. [PubMed: 12824270]

19. Takeda A, et al. CCR3 is a target for age-related macular degeneration diagnosis and therapy. Nature. 2009; 460:225–230. [PubMed: 19525930]

20. Van de Veire S, et al. Further pharmacological and genetic evidence for the efficacy of PlGF inhibition in cancer and eye disease. Cell. 2010; 141:178–190. [PubMed: 20371353]

21. Sun D, Kar S, Carr BI. Differentially expressed genes in TGF-beta 1 sensitive and resistant human hepatoma cells. Cancer Lett. 1995; 89:73–79. [PubMed: 7882305]

22. Li X, Miyajima M, Jiang C, Arai H. Expression of TGF-betas and TGF-beta type II receptor in cerebrospinal fluid of patients with idiopathic normal pressure hydrocephalus. Neurosci Lett. 2007; 413:141–144. [PubMed: 17194537]

23. Saito K, et al. Gene expression profiling of mucosal addressin cell adhesion molecule-1+ high endothelial venule cells (HEV) and identification of a leucine-rich HEV glycoprotein as a HEV marker. J Immunol. 2002; 168:1050–1059. [PubMed: 11801638]

24. Spirin KS, et al. Basement membrane and growth factor gene expression in normal and diabetic human retinas. Curr Eye Res. 1999; 18:490–499. [PubMed: 10435836]

25. Gao BB, Chen X, Timothy N, Aiello LP, Feener EP. Characterization of the vitreous proteome in diabetes without diabetic retinopathy and diabetes with proliferative diabetic retinopathy. J Proteome Res. 2008; 7:2516–2525. [PubMed: 18433156]

26. Anderberg C, et al. Deficiency for endoglin in tumor vasculature weakens the endothelial barrier to metastatic dissemination. J Exp Med. 2013; 210:563–579. [PubMed: 23401487]

27. Mahmoud M, et al. Pathogenesis of arteriovenous malformations in the absence of endoglin. Circ Res. 2010; 106:1425–1433. [PubMed: 20224041]

28. Bobik A. Transforming growth factor-betas and vascular disorders. Arterioscler Thromb Vasc Biol. 2006; 26:1712–1720. [PubMed: 16675726]

29. ten Dijke P, Goumans MJ, Pardali E. Endoglin in angiogenesis and vascular diseases. Angiogenesis. 2008; 11:79–89. [PubMed: 18283546]

30. Lebrin F, et al. Endoglin promotes endothelial cell proliferation and TGF-beta/ALK1 signal transduction. EMBO J. 2004; 23:4018–4028. [PubMed: 15385967]

31. Ray BN, Lee NY, How T, Blobe GC. ALK5 phosphorylation of the endoglin cytoplasmic domain regulates Smad1/5/8 signaling and endothelial cell migration. Carcinogenesis. 2010; 31:435–441. [PubMed: 20042635]

32. Lynch J, et al. MiRNA-335 suppresses neuroblastoma cell invasiveness by direct targeting of multiple genes from the non-canonical TGF-   signalling pathway. Carcinogenesis. 2012; 33:976–985. [PubMed: 22382496]

33. Gregory AD, Capoccia BJ, Woloszynek JR, Link DC. Systemic levels of G-CSF and interleukin-6 determine the angiogenic potential of bone marrow resident monocytes. J Leukoc Biol. 2010; 88:123–31. [PubMed: 20354107]

References

34. Blanks JC, Johnson LV. Vascular atrophy in the retinal degenerative rd mouse. J Comp Neurol. 1986; 254:543–553. [PubMed: 3805362]

35. Heckenlively JR, et al. Mouse model of subretinal neovascularization with choroidal anastomosis. Retina. 2003; 23:518–522. [PubMed: 12972764]

36. McKenzie JA, et al. Apelin is required for non-neovascular remodelling in the retina. Am J Pathol. 2012; 108:399–409. [PubMed: 22067912]

37. Fruttiger M. Development of the mouse retinal vasculature: angiogenesis versus vasculogenesis. Invest Ophthalmol Vis Sci. 2002; 43:522–527. [PubMed: 11818400]

38. Abbott NJ, Hughes CC, Revest PA, Greenwood J. Development and characterisation of a rat brain capillary endothelial culture: towards an in vitro blood-brain barrier. J Cell Sci. 1992; 103:23–37. [PubMed: 1429907]

39. Romero IA, et al. Changes in cytoskeletal and tight junctional proteins correlate with decreased permeability induced by dexamethasone in cultured rat brain endothelial cells. Neurosci Lett. 2003; 344:112–116. [PubMed: 12782340]

40. Arnaoutova I, Kleinman HK. In vitro angiogenesis: endothelial cell tube formation on gelled basement membrane extract. Nat Protoc. 2010; 5:628–635. [PubMed: 20224563]

41. Deckers M, et al. Effect of angiogenic and antiangiogenic compounds on the outgrowth of capillary structures from fetal mouse bone explants. Lab Invest. 2001; 81:5–15. [PubMed: 11204273]

42. Nicosia RF, Ottinetti A. Growth of microvessels in serum-free matrix culture of rat aorta. A quantitative assay of angiogenesis in vitro. Lab Invest. 1990; 63:115–122. [PubMed: 1695694]

43. Balaggan KS, et al. EIAV vector-mediated delivery of endostatin or angiostatin inhibits angiogenesis and vascular hyperpermeability in experimental CNV. Gene Ther. 2006; 13:1153–1165. [PubMed: 16572190]

44. Toma HS, Barnett JM, Penn JS, Kim SJ. Improved assessment of laser-induced choroidal neovascularization. Microvasc Res. 2010; 80:295–302. [PubMed: 20553963]

45. Smith LE, et al. Oxygen-induced retinopathy in the mouse. Invest Ophthalmol Vis Sci. 1994; 35:101–111. [PubMed: 7507904]

46. Connor KM, et al. Quantification of oxygen-induced retinopathy in the mouse: a model of vessel loss, vessel regrowth and pathological angiogenesis. Nat Protoc. 2009; 4:1565–1573. [PubMed: 19816419]
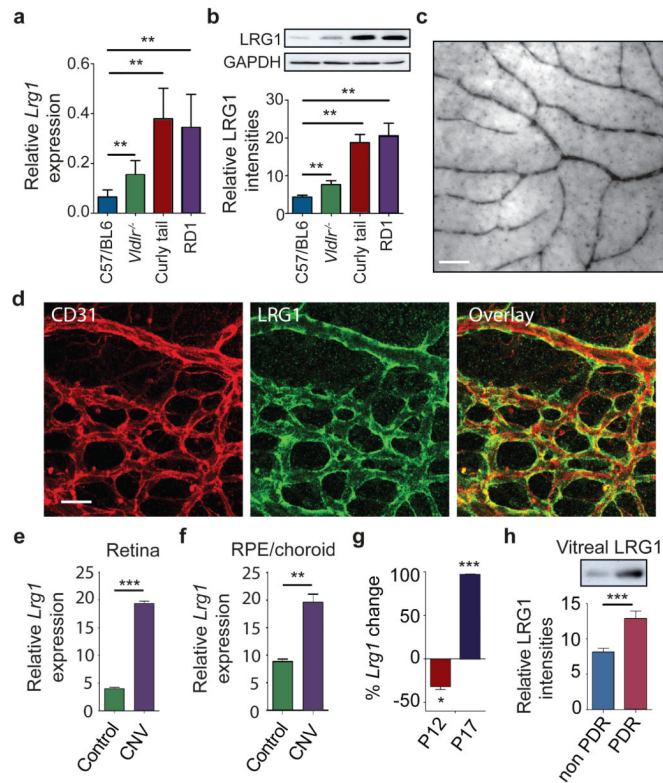
**Figure 1. LRG1 is over-expressed in pathogenic retinal vasculature**
a, Quantification of *Lrg1* mRNA and **b**, LRG1 protein expression showing up-regulation in the retina of mice exhibiting retinal vascular changes. **c**, *Lrg1 in situ* hybridisation at P21. Scale bar = 50μm. **d**, Immunohistochemical detection of CD31 (red) and LRG1 (green) at P10 showing LRG1 expression in the retinal vasculature. **e**, Up-regulation of *Lrg1* mRNA in the retina and **f**, RPE/choroid in CNV mice. **g**, Reduced *Lrg1* transcript levels in OIR at P12 and increased levels at P17. **h**, Elevation of LRG1 protein in the vitreous of patients with PDR. All images shown are representative and values are expressed as means ± s.e.m of 3 independent experimental groups. *$P<0.05$, **$P<0.01$, ***$P<0.001$.
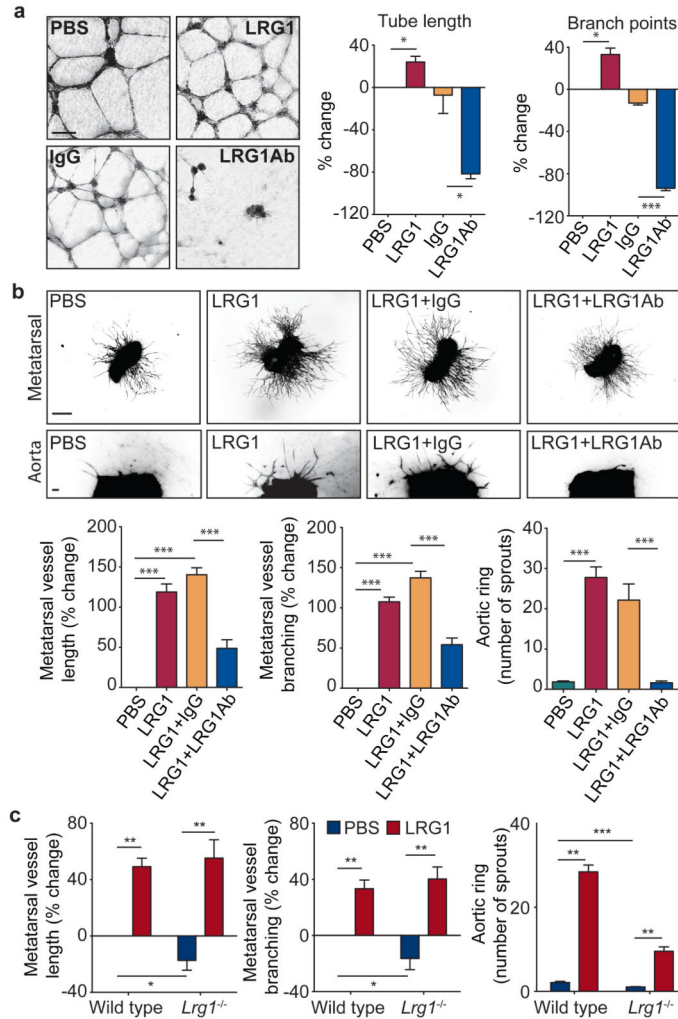
Figure 2. LRG1 promotes angiogenesis

a, Increased HUVEC tube and branch formation following addition of LRG1 and inhibition by a LRG1 neutralizing antibody. Scale bar 160μm. **b**, Vessel outgrowth in the metatarsal (top row) and aortic ring (bottom row) assay is enhanced by LRG1 and attenuated by a LRG1 neutralizing antibody. Scale bar = 1,500μm. **c**, Comparison of vessel growth from metatarsals and aortic rings isolated from WT and $Lrg1^{-/-}$ mice shows reduced angiogenesis in the latter that could be rescued by the addition of LRG1. All images shown are representative and values are expressed as means ± s.e.m of n ≥ 3 independent experimental groups. *P<0.05, **P<0.01, ***P<0.001.
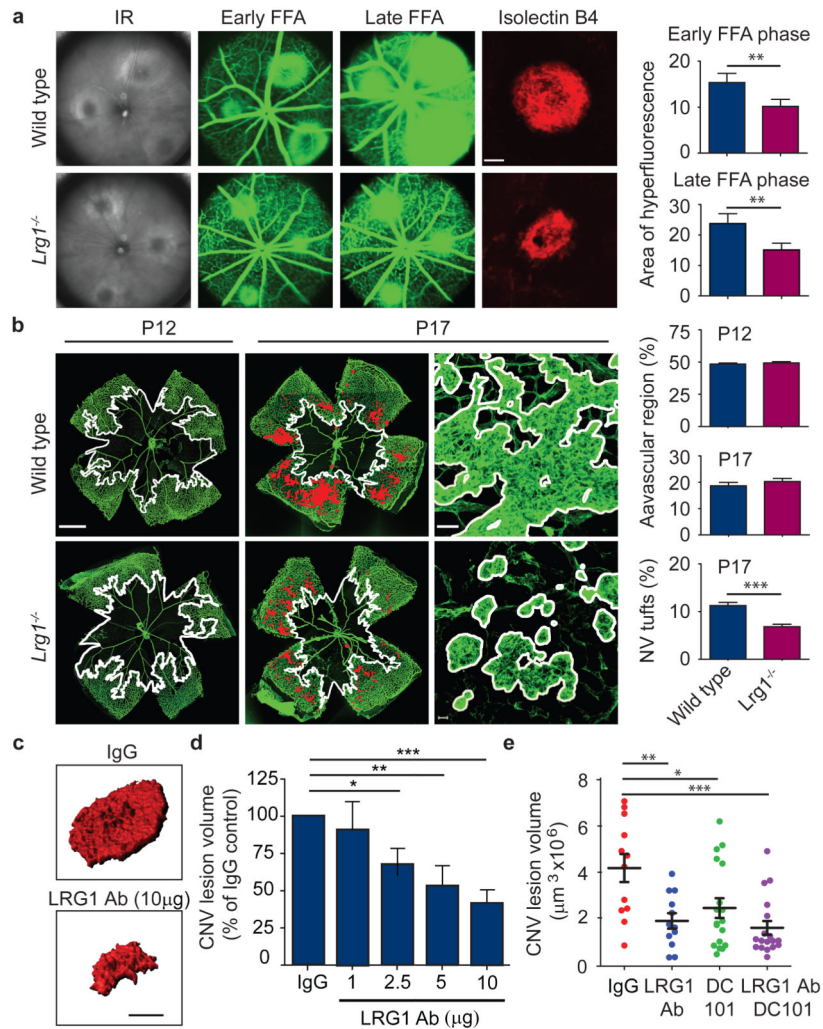
Figure 3. Lrg1 contributes to pathogenic neovascularisation
a, Representative images of WT and *Lrg1*$^{-/-}$ mouse laser-burn lesions by infra red (IR) fundus imaging. At 7 days post laser, early and late-phase fundus fluorescein angiography (FFA) revealed a reduction in CNV lesion size and a decrease in fluorescein leakage respectively in *Lrg1*$^{-/-}$ mice. Representative images of isolectin B4 stained (red) CNV in choroidal/RPE flat-mount 7 days after induction confirming decreased lesion size in *Lrg1*$^{-/-}$ mice. Scale bar = 100μm. **b**, In OIR *Lrg1* deletion does not affect the size of the avascular region at P12 (delineated by white boundary line) or the organised normal revascularisation at P17 (scale bar = 1000μm) but does decrease the formation of pathological neovascular (NV) tufts (highlighted in red and delineated in higher power by white boundary line). Scale bar = 50μm. **c**, Volume-rendered examples of PECAM-1 stained CNV lesions in WT mice following intravitreal injection of irrelevant IgG or LRG1 neutralising antibody (scale bar = 100μm). **d**, Dose-dependent anti-LRG1 antibody reduction of CNV lesion volume. **e**, Combination of anti-LRG1 and DC101 (anti-VEGFR2) in CNV in WT mice resulted in enhanced reduction of lesion volume compared to single treatments. All values represent means ± s.e.m of n ≥ 10 for each group. *P<0.05; **P<0.01; ***P<0.001.
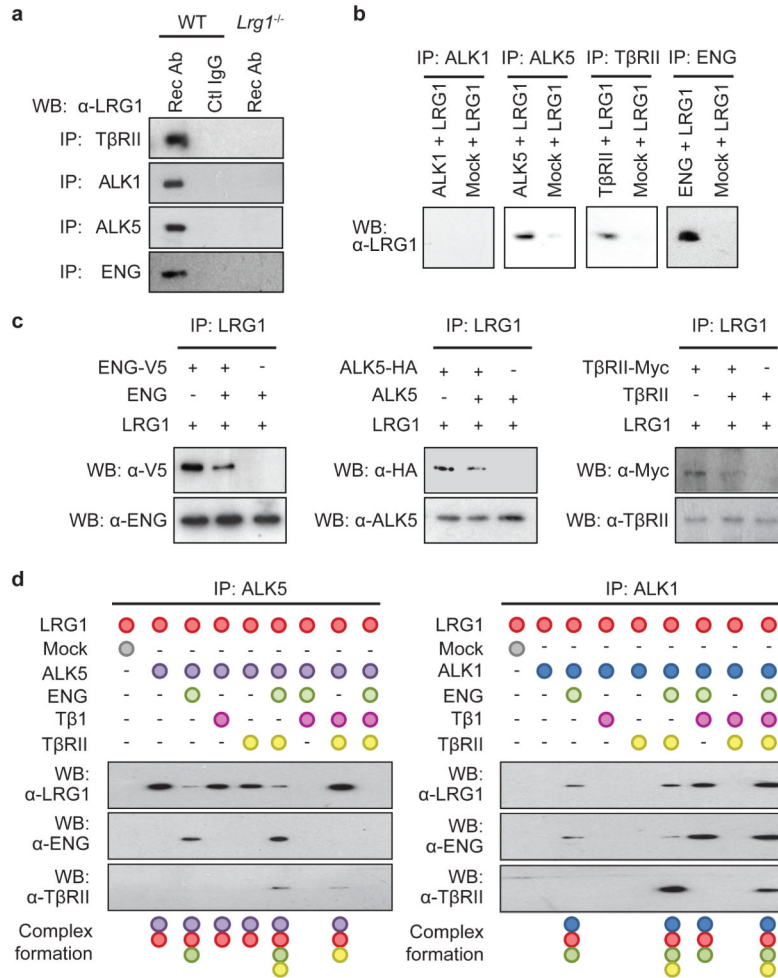
Figure 4. LRG1 modifies the TGFβ receptor complex

a, Immunoprecipitation of TβRII, ALK1, ALK5 and ENG with anti-receptor antibodies (Rec Ab) from WT mouse brain EC lysates co-precipitates LRG1. Control IgG in WT ECs or Rec Ab in *Lrg1*⁻/⁻ ECs did not co-precipitate LRG1. **b**, Immunoprecipitation of peptide-tagged extracellular domains of ALK5 (HA-tagged), TβRII (Myc-tagged) or ENG (V5-tagged) added individually to His-tagged LRG1 resulted in co-precipitation of LRG1 indicating direct interactions with these receptors. Immunoprecipitation of ALK1 (HA-tagged) in the presence of LRG1 did not co-precipitate the latter. **c**, Addition of appropriate soluble non-tagged extracellular domains of ENG, ALK5 and TβRII competed off peptide-tagged receptor binding to LRG1. **d**, LRG1 was incubated *in vitro* with different combinations of TGFβ receptor extracellular domains and TGFβ1. In the presence of ENG binding between LRG1 and ALK5 is diminished and with the further addition of TGFβ1 is completely lost. Conversely, ENG facilitates the association between LRG1 and ALK1, which is enhanced in the presence of TGFβ1. Although TβRII has no impact on LRG1/ALK1 or LRG1/ALK5 interactions, it is recruited to the complex in the presence of ENG. All data are representative western blots of n ≥ 3 for each experiment.
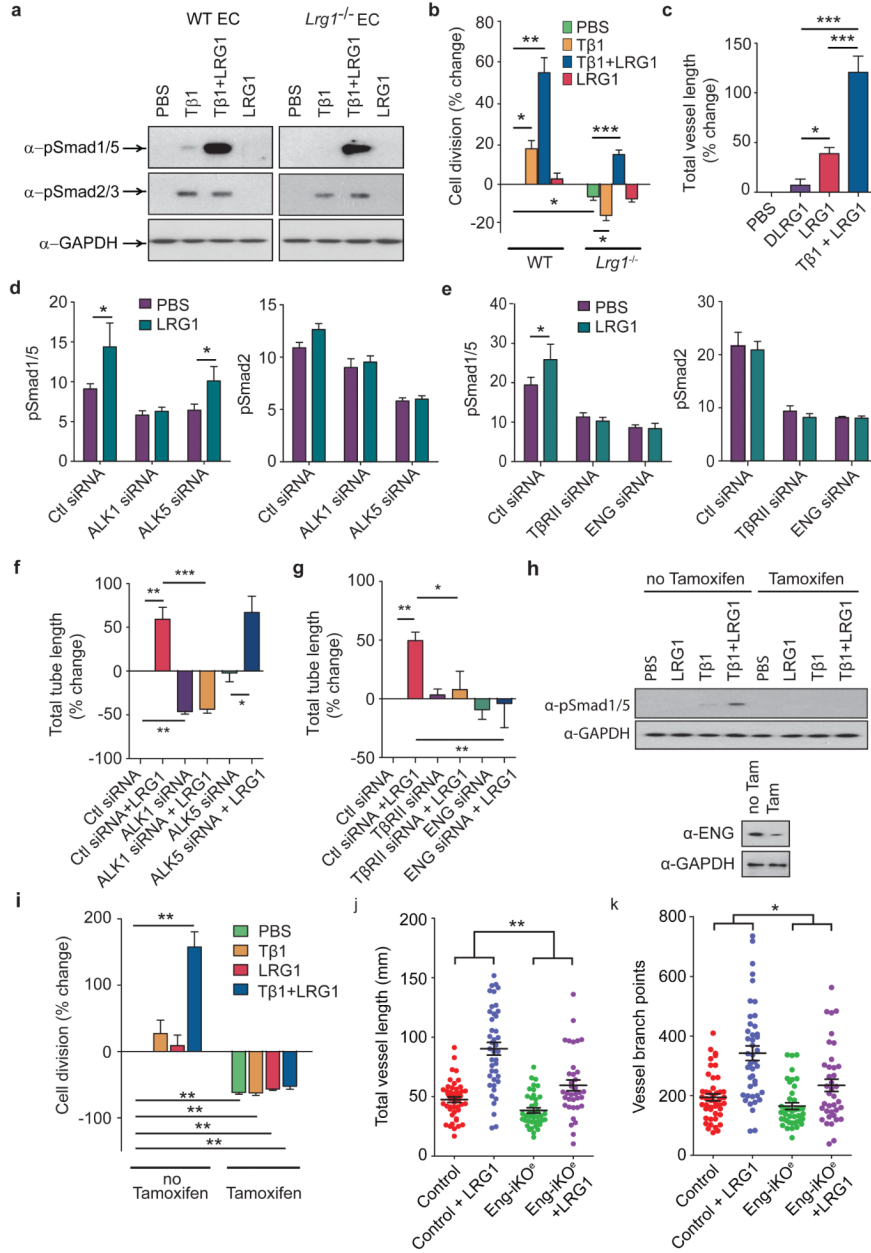
Figure 5. LRG1 promotes angiogenesis via a switch in TGFβ signalling
a, In WT brain ECs, TGFβ1 (Tβ1) stimulates Smad 2/3 phosphorylation and low levels of Smad 1/5 phosphorylation but in *Lrg1*−/− brain ECs only Smad 2/3 is phosphorylated. Addition of LRG1 has no effect on Smad phosphorylation in WT or *Lrg1* null cells but co-treatment with TGFβ1 and LRG1 enhances Smad 1/5 phosphorylation without affecting Smad2/3 phosphorylation (n ≥ 3). **b**, Proliferation of brain ECs isolated from WT control and *Lrg1*−/− mice after exogenous TGFβ1 and/or LRG1 treatment normalized to control (n ≥ 3). Non-treated *Lrg1*−/− ECs are less proliferative than WT ECs. Addition of TGFβ1 to WT ECs results in enhanced proliferation but reduces proliferation in *Lrg1*−/− ECs whereas TGFβ1 and LRG1 co-treatment results in enhanced proliferation in WT and *Lrg1*−/− ECs. **c**,

Addition of exogenous TGF 1 and LRG1, compared to LRG1 alone or denatured (D)LRG1, enhances microvessel formation in the mouse metatarsal angiogenesis assay (n=3 independent experiments, n 30 metatarsals per treatment). **d**, siRNA knockdown of ALK1 or ALK5 in HUVEC results in reduced Smad1/5 and Smad2 phosphorylation respectively. ALK1, but not ALK5, knockdown results in prevention of LRG1-induced Smad1/5 phosphorylation. Histograms show semi-quantification of Smad phosphorylation relative to GAPDH (n 3). **e**, siRNA knockdown of T RII or ENG inhibits LRG1-induced Smad1/5 phosphorylation. Histograms show semi-quantification of Smad phosphorylation relative to GAPDH (n 3). **f** and **g**, Knockdown of ALK1, T RII or ENG, but not ALK5, reduces LRG1-mediated HUVEC Matrigel tube formation. (n=3 independent groups for each assay). **h**, Treatment of lung ECs isolated from *Rosa26-CreERT:Eng*$^{fl/fl}$ mice (MLEC;*Eng*$^{fl/fl}$) with a combination of TGF 1 and LRG1 results in Smad 1/5 phosphorylation, whereas following pre-treatment with 4OH-tamoxifen to delete ENG (MLEC;*Eng*$^{-/-}$) the response is lost. **i**, Treatment of MLEC;*Eng*$^{fl/fl}$ with a combination of TGF 1 and LRG1 stimulates cell division. In MLEC;*Eng*$^{-/-}$ cell division is reduced and refractive to treatment with TGF 1 ± LRG1 (n=3 independent experiments). **j,** 4OH-tamoxifen treatment of metatarsals isolated from *Eng*$^{fl/fl}$ (control) and *Cdh5(PAC)-CreERT2;Eng*$^{fl/fl}$ (Eng-iKO^e) mice results in loss of ENG expression in the latter (Supplementary Fig 30) and decreases LRG1 induced metatarsal vessel length and **k**, vessel branching (metatarsals from 5 independent litters). All values represent means ± s.e.m. * $P<0.05$; ** $P<0.01$; *** $P<0.001$.